Supplementary Information

Hierarchical Nested Wrinkles on Silica−Polymer Hybrid Films: Stimuli-Responsive Micro Periodic Surface Architectures

Yasuaki Tokudome, Kazumasa Suzuki, Takuya Kitanaga, and Masahide Takahashi

Supplementary Note:

Note S1. Glow-discharge optical emission spectroscopy (GD-OES) analysis. The nominal mass ratio of starting components gives a C/Si ratio of 13.9, supposing that solvent evaporation and hydrolysis of TEOS proceed completely. C sources: PVP, AM, 4,4′-Bis(dimethylamino)benzophenone; Si source: TEOS. The difference between the measured and calculated C/Si ratios arises because the reactions are incomplete, as is typical for sol-gel derived films.

Supplementary Method:

Method S1. Size selective adsorption surface for micrometre-sized particles. Polydisperse polystyrene particles with a concentration of 1% and nominal diameter range of 2–15 μm, dispersed in water (LD10, Thermo Fisher Scientific Inc.), were centrifuged. The water was decanted, and the pellet redispersed in ethanol. Then, a glass substrate on which a nested wrinkle structure had been formed was dipped into the ethanolic polystyrene colloids. The substrate was pulled out from the solution, dried, and then examined using an optical microscope. On the observed image (355 μm × 266 μm), particles within individual size scales were tallied to obtain the particle size distribution.

Supplementary Figures:
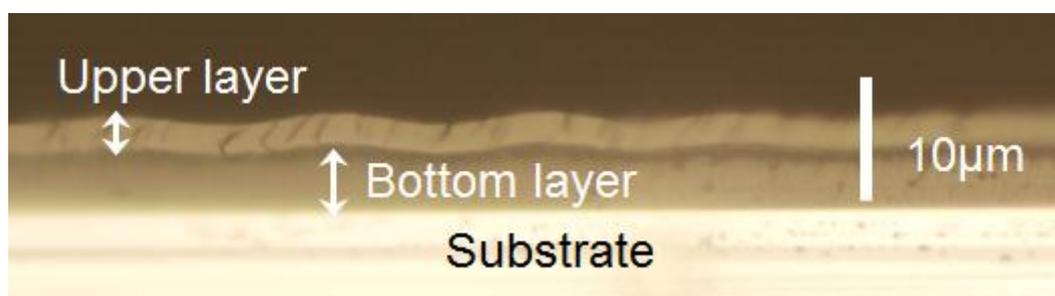
Fig. S1 Bilayer structure formed on a substrate. A fractured surface of the wrinkle structure prepared on a Si substrate using a spinning rate of 2000 rpm. A bilayer structure with total thickness of ~8 μm was obtained.
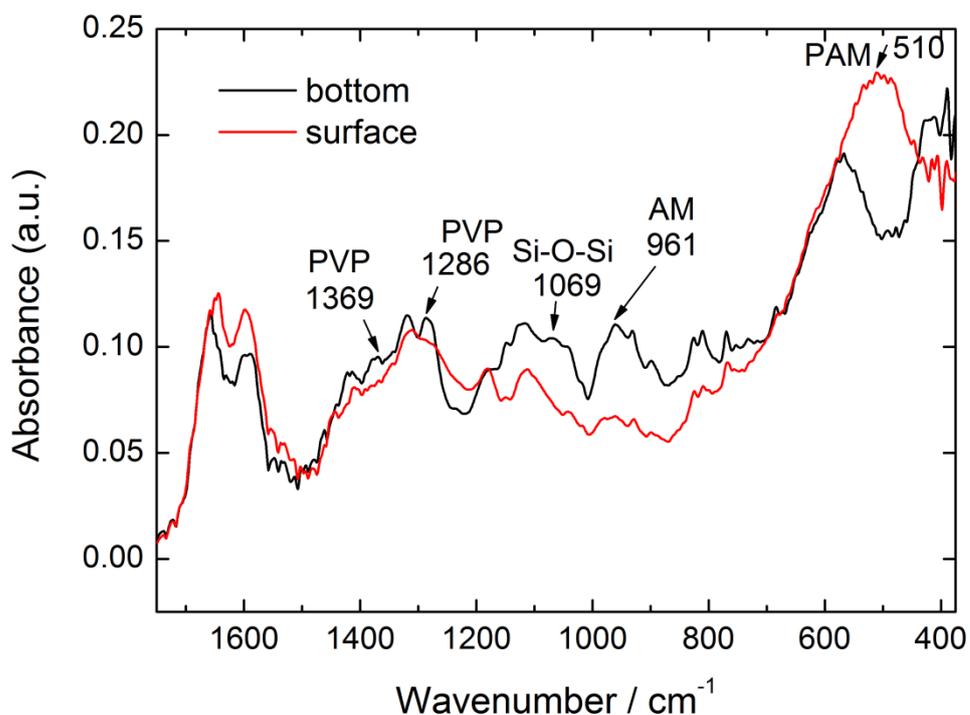
Fig. S2 Compositional difference between surface and bottom parts of the bilayer film.
Attenuated total reflectance (ATR) FT-IR spectra of the surface and bottom layers of the bilayer film. After UV-curing, the film surface was analyzed, and then the surface part was peeled away, and the bottom part was analyzed. The penetration depth of the incident IR (defined as the length at which incident light intensity equals 1/e of that at the surface) was estimated as 3.2 μm at 1000 cm^{-1} using an incident angle of 45°. Although the spectra from one layer of the film can include some contribution from the other layer, the components of the respective layers were qualitatively investigated (See Fig. 3b for the more detailed depth profiles of the components). Some peaks from the constituents are overlapped. Peak assignment was performed on clearly-identifiable bands; the bands at 961 and 1069 cm^{-1} correspond to the =CH$_2$ wagging vibration of AM and the stretching vibration of Si-O-Si, respectively; the broad band at 510 cm^{-1} is characteristic of poly(acrylamide) (PAM); the bands at 1286 and 1369 cm^{-1} can be ascribed to PVP.[1-4] The PAM is mainly distributed in the surface layer, whereas PVP and silica together with residual AM are predominantly in the bottom layer.
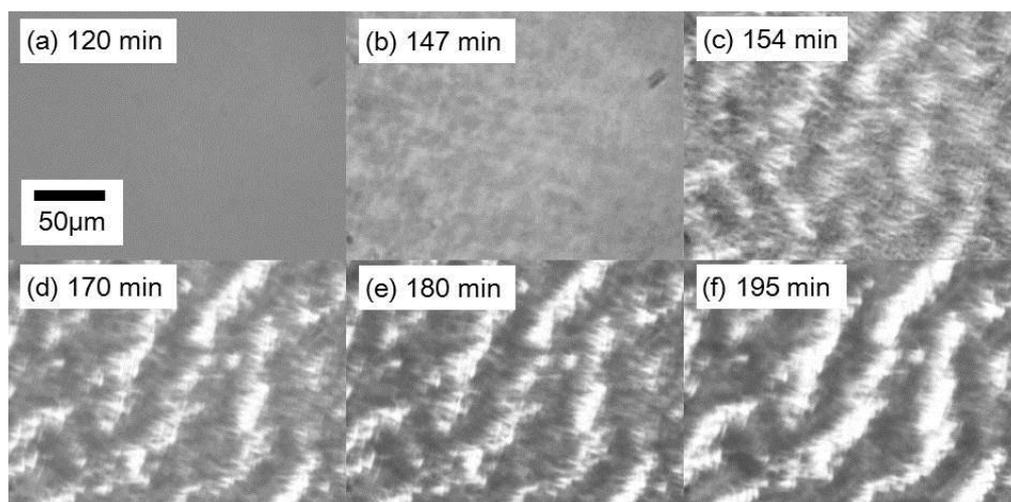
Fig. S3 Time evolution of NW structure formation. The film was coated onto a glass substrate using a spinning rate of 1000 rpm, and the wrinkle formation process was followed. The reaction time is the time elapsed after coating.
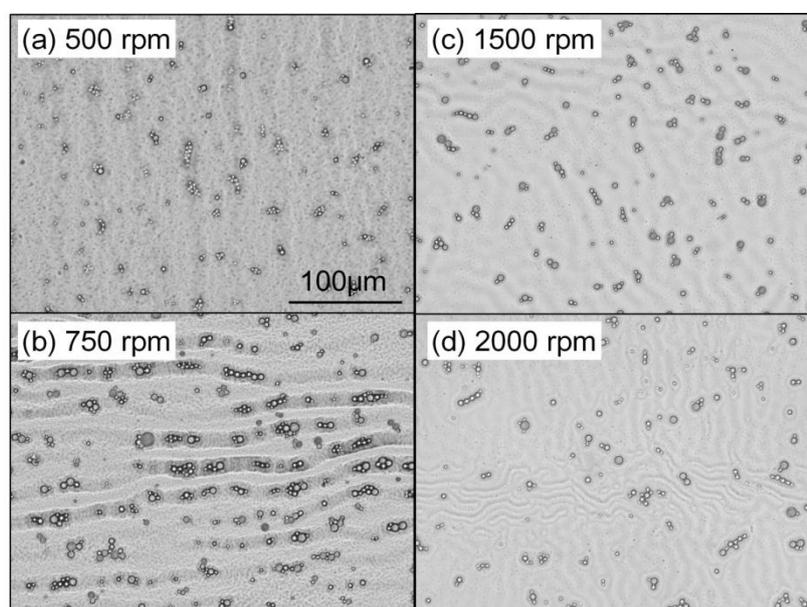
Fig. S4 Particles selectively captured by wrinkles. Optical microscope images showing particles captured by wrinkles on films coated at spinning rates of (a) 500 rpm, (b) 750 rpm, (c)1500 rpm, and (d) 2000 rpm.
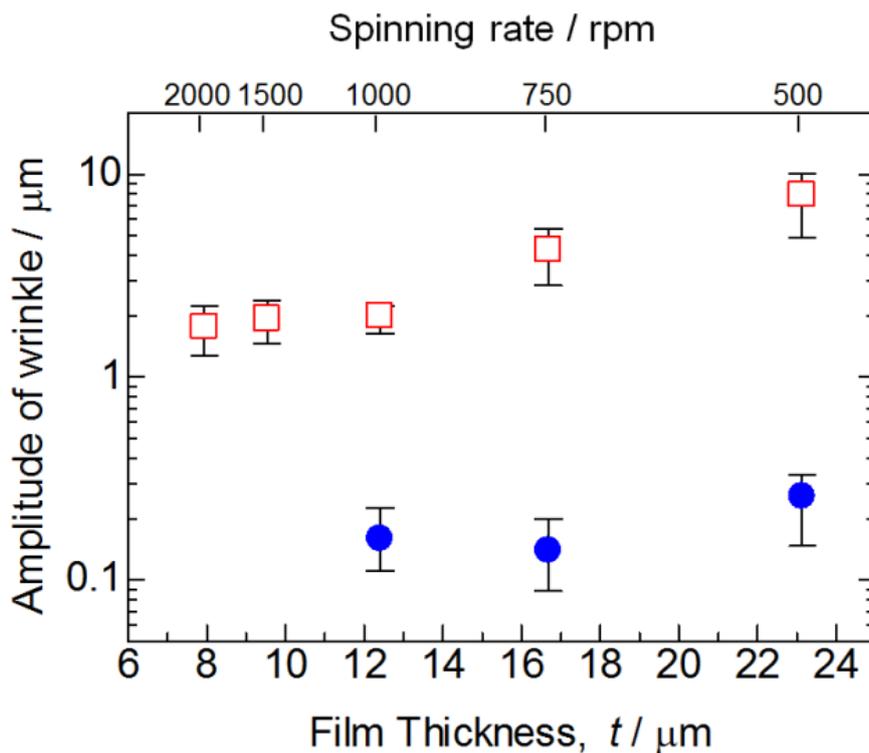
Fig. S5 Tunability of amplitude of wrinkle structures. Dependence of amplitude of wrinkle structures on total film thickness; □ (red): 2G structure; ● (blue): 1G structure. Coatings were made on glass substrates. Corresponding spinning rates for the respective film thicknesses are depicted on the upper axis. The analysis was performed from 3D images taken with laser scanning confocal microscopy (LSCM). The amplitude of the wrinkles was measured at 10 different points and averaged for each sample. For the spinning rate of 1500 rpm (t = 9.5 μm), the amplitude of the 1G structure was too small to be detected with LSCM. No 1G-wrinkle was formed at 2000 rpm (t = 7.9 μm). The amplitude of the 2G structure increases with total film thickness. The amplitude of the 1G structure was also expected to increase with total film thickness;[5] however, this trend was not observed in this study, presumably because of the relatively large errors that can occur in the analysis of NW structures.
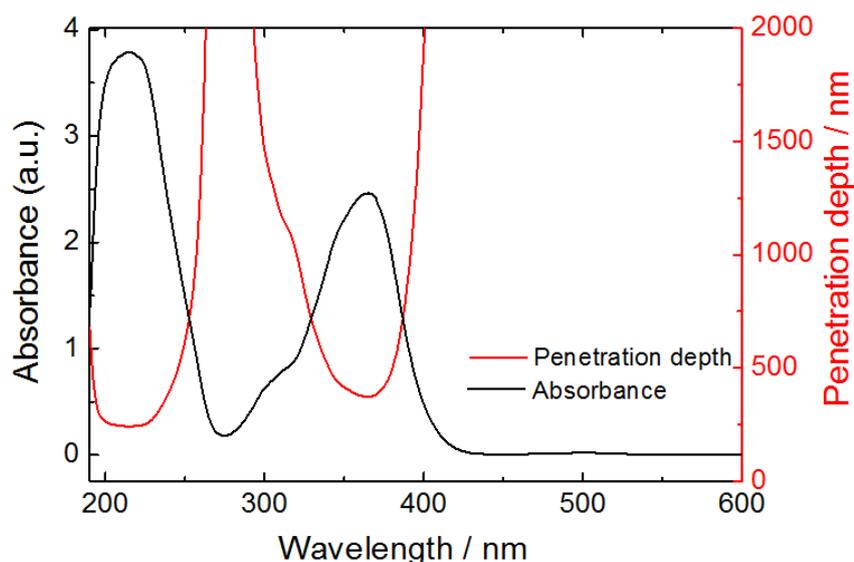
Fig. S6 Estimation of depth of penetration of irradiated UV light into spin-coated films. (Black line) UV-Vis absorption spectrum of the coating solution diluted 400 times with ethanol. (Red line) penetration depth of incident light, λ =254 nm, as estimated for the coating solution from the Beer-Lambert law. The molar absorption coefficient obtained from UV-Vis measurements was used for the calculation, setting (I/I_0) at 1/e, where I and I_0 are transmitted light intensity and incident light intensity, respectively.

References

1. Orcel, G., Phalippou, J., Hench, L. L. Structural changes of silica xerogels during low temperature dehydration. *J. Non-Cryst. Solids* **88**, 114−130 (1986).
2. Dirè, S., *et al.* Hydroxylated cyclophosphazene/silica hybrid materials: synthesis and characterization. *J. Inorg. Organomet. Polym.* **12**, 59−78 (2002).
3. Kolek, E., Šimko, P., Šimon, P., Gatial, A. Confirmation of polymerisation effects of sodium chloride and its additives on acrylamide by infrared spectrometry. *J. Food Nutr. Res.* **46**, 39−44 (2007).
4. Oh, T.-J., Nam, J.-H., Jung, Y. M. Molecular miscible blend of poly(2-cyano-1,4-phenyleneterephthalamide) and polyvinylpyrrolidone characterized by two-dimensional correlation FTIR and solid state ^{13}C NMR spectroscopy. *Vib. Spectrosc.* **51**, 15−21 (2009).
5. Cerda, E., Mahadevan, L. Geometry and physics of wrinkling. *Phys. Rev. Lett.* **90**, 074302 (2003).